HHS Public Access

Author manuscript

Hepatology. Author manuscript; available in PMC 2017 March 01.

Published in final edited form as:

Hepatology. 2016 March ; 63(3): 731–744. doi:10.1002/hep.28252.

Mixed Lineage Kinase 3 Mediates Release of C-X-C Motif Ligand 10-Bearing Chemotactic Extracellular Vesicles from Lipotoxic Hepatocytes

Samar H. Ibrahim[1], **Petra Hirsova**[2], **Kyoko Tomita**[2], **Steven F. Bronk**[2], **Nathan W. Werneburg**[2], **Stephen A. Harrison**[3], **Val S. Goodfellow**[4], **Harmeet Malhi**[2], and **Gregory J. Gores**[2]

Samar H. Ibrahim: Ibrahim.samar@mayo.edu; Petra Hirsova: Hirsova.petra@mayo.edu; Kyoko Tomita: tomita.kyoko@mayo.edu; Steven F. Bronk: bronk.steven@mayo.edu; Nathan W. Werneburg: werneberg.nathan@mayo.edu; Stephen A. Harrison: stephen.a.harrison.mil@mail.mil; Val S. Goodfellow: vsgoodfellow@califiabio.com; Harmeet Malhi: Malhi.harmeet@mayo.edu; Gregory J. Gores: gores.gregory@mayo.edu

[1]Division of Pediatric Gastroenterology, Mayo Clinic, Rochester, Minnesota

[2]Division of Gastroenterology & Hepatology, Mayo Clinic, Rochester, Minnesota

[3]Brooke Army Medical Center, Fort Sam Houston, TX

[4]Califia Bio, Inc., San Diego, CA

Abstract

Background and aims—Mixed lineage kinase 3 (MLK3) deficiency reduces macrophage associated-inflammation in a murine model of nonalcoholic steatohepatitis (NASH). However, the mechanistic links between MLK3 activation in hepatocytes and macrophage-driven inflammation in NASH are uncharted. Herein, we report that MLK3 mediates the release of (C-X-C motif) ligand 10 (CXCL10)-laden extracellular vesicles (EVs) from lipotoxic hepatocytes, which induce macrophage chemotaxis.

Methods—Primary mouse hepatocytes (PMH) and Huh7 cells were treated with palmitate or lysophosphatidylcholine (LPC). Released EVs were isolated by differential ultracentrifugation.

Results—LPC treatment of PMH or Huh7 cells induced release of EVs, which was prevented by either genetic or pharmacological inhibition of MLK3. Mass spectrometry identified the potent chemokine CXCL10 in the EVs, which was markedly enriched in EVs isolated from LPC-treated hepatocytes versus untreated cells. Green fluorescent protein (GFP)-tagged CXCL10 was present in vesicular structures and co-localized with the red fluorescent protein (RFP)-tagged EV marker cluster of differentiation (CD) 63 following LPC treatment of co-transfected Huh-7 cells. Either genetic deletion or pharmacological inhibition of MLK3 prevented CXCL10 enrichment in EVs.

Contact Information: Gregory J. Gores, MD, Professor of Medicine and Physiology, Mayo Clinic, 200 First Street SW, Rochester, Minnesota 55905, Tel: 507 284 0686; Fax: 507 284 0762, gores.gregory@mayo.edu.

Conflict of Interest: The authors report no conflict of interest.

Financial Disclosure: The authors have no financial disclosures.

Author Contributions: S.H.I., P.H., S.F.B., N.W.W., K.T. designed and performed experiments and acquired and analyzed data. V.S.G., H.M., S. A. H. Provided material support and contributed to manuscript preparation. S.H.I. and G.J.G. conceptualized the study, designed experiments, analyzed and interpreted data and prepared the manuscript.

Treatment of mouse bone marrow-derived macrophages with lipotoxic hepatocyte-derived EVs induced macrophage chemotaxis, an effect blocked by incubation with CXCL10 neutralizing antisera. MLK3 deficient mice fed a NASH-inducing diet had reduced concentrations of total plasma EVs, and CXCL10 containing EVs compared to WT mice.

In Conclusion—during hepatocyte lipotoxicity, activated MLK3 induces the release of CXCL10-bearing vesicles from hepatocytes, which are chemotactic for macrophages.

Keywords

nanoparticles; lipotoxicity; nonalcoholic steatohepatitis; macrophage; chemotaxis

Nonalcoholic fatty liver disease is present in up to 30% of the American population (1). A subset of these individuals develops hepatic inflammation, referred to as nonalcoholic steatohepatitis (NASH) (2), which can progress to cirrhosis and its sequelae of end stage liver disease (3, 4). NASH has become a significant public health problem lacking regulatory agency-approved pharmacotherapy. Hence, a better understanding of the molecular and cellular mechanisms involved in the pathogenesis of NASH development and progression may facilitate identification of specific therapeutic targets.

NASH is a lipotoxic disorder and current concepts suggest that saturated free fatty acids (SFA)s participate in hepatocyte lipotoxicity (5, 6). SFA metabolism to lysophosphatidylcholine (LPC), in part, contributes to lipoapoptosis (7, 8). Hepatocyte lipoapoptosis is the pathogenic hallmark of NASH and correlates with disease severity (9). C-JUN N-terminal kinase (JNK) activation is crucial in the development of hepatocyte apoptosis accompanying NASH (10). Mixed lineage kinase 3 (MLK3) is the mitogen-activated protein kinase (MAPK) that mediates SFAs-induced JNK activation in the liver (11). The role of MLK3 as a proapoptotic kinase has been established in different models of cell injury (12–14) and, accordingly, we have recently reported that *Mlk3*$^{-/-}$ mice are protected against liver injury in NASH-inducing diet (15).

Influx and activation of macrophages within the liver is an essential pathogenic process in the progression of nonalcoholic fatty liver disease (16). Hepatic macrophages promote NASH development by the production of pro-inflammatory cytokines such as tumor necrosis factor (TNF) α, Interleukin (IL) 1 and IL6 (16). The high fat and carbohydrate diet-fed *Mlk3*$^{-/-}$ mice have decreased macrophages infiltration, and cytokines expression in their liver, compared to wild type (WT) animals on the same diet (15). However, the mechanism by which hepatocyte lipotoxicity results in macrophage chemotaxis and activation within the liver is unclear.

Cells release into the extracellular environment diverse types of membrane bound vesicles of endosomal and plasma membrane origin termed exosomes and microvesicles, respectively, and extracellular vesicles (EVs) collectively. These EVs act as vectors of information that regulate the function of target cells (17). Liver cells are EVs-releasing cells as well as targets for endogenous EVs. Initial observations suggest that EVs are important in liver pathophysiology through mediating intercellular signaling (18). Repeated injection of EVs isolated from the serum of high fat diet-fed mice into regular diet-fed mice resulted in

accumulation of activated immature myeloid cells in the liver, and enhanced fatty liver disease (19). The missing link between hepatocyte lipotoxic injury and development of macrophage-associated inflammation lead us to propose that proapoptotic lipotoxic signaling by MLK3 may induce release of proinflammatory EVs from hepatocytes, which, in turn, induce macrophage chemotaxis. A likely process mediating this intercellular communication would be release of chemokine-bearing EVs from hepatocytes, which then stimulate macrophages trafficking to the liver.

The (C-X-C motif) ligand 10 (CXCL10) is upregulated in patients with various types of chronic liver disease and the increase correlates with the severity of liver fibrosis (20). More importantly, CXCL10 was recently found to be upregulated in NASH patients and to contribute to the pathogenesis of methionine and choline-deficient diet-induced NASH through regulation of lipogenesis and oxidative stress (21). Although the mechanisms regulating CXCL10 expression in NASH are largely unknown; signal transducer and activator of transcription (STAT) 1, a transcription factor known to induce inflammatory and immune response, was reported to bind to the CXCL10 promoter, and mediate its induction (22). Hence, STAT1 is a potential mediator of CXCL10 upregulation in NASH. Although CXCL10 is a secreted chemokine, CXCL10 structure supports the formation of higher order oligomers (23), CXCL10 is known to bind to glycosaminoglycans which is required for the biological function of the chemokine, mostly by facilitating its oligomerization, a requisite step for its *in vivo* activity (23). Interestingly, proteins oligomerization has been shown to promote their packaging into EVs (24). The regulation of CXCL10 release by lipotoxic insults and its potential localization within EVs remain undefined. Herein, we report that toxic lipids, indeed, promote release of EVs from hepatocytes by an MLK3 signaling cascade. We report that lipotoxic hepatocyte-derived EVs are enriched with the potent chemotactic ligand CXCL10, which in turn, induces macrophage chemotaxis. In a murine model of NASH, genetic deficiency in MLK3 is protective against liver injury and is associated with a decrease in the number of CXCL10 bearing EVs in the circulation, and macrophage-associated hepatic inflammation. These findings mechanistically integrate hepatocyte lipotoxicity and inflammation in NASH, and further implicate EVs in hepatocyte to macrophage signaling cascades.

EXPERIMENTAL PROCEDURES

Extracellular vesicle isolation

PMH and Huh7 cells were washed twice with phosphate buffer solution (PBS) to eliminate fetal bovine serum (FBS)-derived EVs, and treated with either 20 μM LPC for 4 hours with or without one of the MLK3 inhibitors, 400 μM palmitate (PA), or oleate (OA) for 16 hours, or vehicle in serum-free medium. EVs were isolated from cell culture medium by differential ultracentrifugation according to a modified protocol by Thery at al. (25). Collected medium was depleted of cells and cell debris initially by low-speed centrifugations (2,000 g for 20 minutes and 20,000 g, for 30 minutes). The supernatants were collected and centrifuged for 90 minutes at 100,000 g at 4 °C. Pellets from this centrifugation step were washed in PBS, and centrifuged again for 90 minutes at 100,000 g at 4 °C. The obtained pellets were lysed in lysis buffer, or re-suspended in PBS solution or

RPMI 1640 medium, depending on the subsequent experiments. EVs used for macrophages treatment were sterile filtered through 0.22 μm syringe filter. EVs isolation was also performed using a commercially available kit from Invitrogen (Carlsbad, CA).

Nanoparticle tracking analysis

Concentration and size distribution of isolated EVs were assessed by nanoparticle tracking analysis (NTA) using NanoSight NS300 instrument (NanoSight Ltd., Amesbury, UK) (26). EV samples were diluted with PBS. Each sample was continuously run through a flow-cell top-plate set up to 23.3°C using a syringe pump at a rate of 25 μl/minute. At least three videos of 30 seconds documenting Brownian motion of nanoparticles were recorded, and at least 1000 completed tracks were analyzed by the NanoSight software (NTA 2.3.5).

Transient transfection of CXCL10-green fluorescent protein (GFP) and cluster of differentiation (CD) 63-red fluorescent protein (RFP), total internal reflection microscopy (TIRF) and confocal microscopy

Huh7 cells were grown in 35-mm dishes and transiently transfected with CXCL10-GFP tagged plasmid (RG203141, Origene, Rockville, MD), and CD63-RFP tagged plasmid (kindly provided by Dr. Mark McNiven, Rochester, MN) using lipofectamin 2000 (Life technology, Grand Island, NY) per manufacturer's instructions. Forty eight hours after transfection, cells were subsequently imaged on a live stage by TIRF microscopy (Axiovert 200M; Zeiss) and LSM780 confocal fluorescence microscope (Carl Zeiss, Jena, Germany), using excitation and emission wavelengths of 488 and 507 nm for GFP and 577 and 590 nm for RFP, respectively. TIRF microscopy only images fluorescence within 100 nm of the cell surface contact area (i.e., contact area between cell and coverslip) (27) and is commonly used to monitor movement of fluorescent molecules from and to the plasma membrane (28).

Additional detailed materials, methods and statistical analysis are provided in the supportive experimental procedures.

RESULTS

Lipotoxic hepatocytes release EVs by an MLK3 dependent pathway

PMH and Huh7 cells were treated with the saturated free fatty acid palmitate (C16:0), its active intracellular metabolite LPC (8) or the non-toxic monounsaturated free fatty acid oleate (C18:1). Secreted EVs were isolated from the cell culture media by ultracentrifugation and quantified by NTA. Size distribution of PMH-derived vesicles was 40–300 nm with a mode size of approximately 85 nm (Fig. 1A), which was also observed by electron microscopy (Fig. 1B). Over a four-hour incubation period, LPC (20 μM) induced a 3-fold increase in release of EVs from PMH (Fig. 1C and D). Interestingly, Huh7 cells treated with LPC demonstrated an even more robust increase in released EVs (Fig 1E). The toxic SFA palmitate (400 μM for 16 hours) also induced release of EVs from PMH (Fig. 1F), whereas, treatment with the nontoxic monounsaturated fatty acid oleate did not (Fig. 1F). The release of EVs from PMH occurred before the onset of apoptosis (Supplemental Figure 1A); therefore, excluding apoptotic bodies from the population of isolated vesicles. The increase in EV release induced by LPC in PMH was repressed in *Mlk3*$^{-/-}$ hepatocytes

(Fig. 1C and D) and also in Huh7 cells incubated with the pharmacological MLK3 inhibitors URMC099 and CLFB1134 (Fig. 1E). MLK3 genetic and pharmacologic inhibition is also protective against LPC induced hepatocyte lipoapoptosis (Supplemental figure 1A and B). MLK3 activates JNK during lipotoxic insults (11), and consistent with these observations, the JNK inhibitor SP600125 also reduced LPC-stimulated release of EVs (Fig. 1E). Immunoblot analysis indicated that isolated EVs contained established EV markers such as tumor susceptibility gene 101 (TSG101), CD63, and ALG-2-interacting protein (Alix) (29) (Fig. 2A). Collectively, these data indicate that toxic lipids induce EV release from human and mouse hepatocytes, which is attenuated by genetic or pharmacological MLK3 inhibition.

CXCL10 is partitioned into lipotoxic EVs by an MLK3-dependent mechanism

We performed mass spectrometry on EVs isolated from vehicle and LPC treated PMH, and identified the potent chemokine CXCL10 as cargo. The presence of CXCL10 as vesicular cargo was readily confirmed by western blot analysis (Fig. 2A) and immunogold electron microscopy (Fig. 2B). CXCL10 associated with EVs was increased by LPC treatment and attenuated in EVs derived from *Mlk3*$^{-/-}$ hepatocytes, or Huh7 cells treated with LPC in the presence of one of the MLK3 inhibitors. In addition, the mass spectrometry demonstrated that EVs from PMH contain cytochrome p450 2E1 (CYP2E1), and since CYP2E1 is only expressed by hepatocytes (30), CYP2E1 can be considered a biomarker for EVs of hepatocyte origin (Fig. 2A). Consistent with the known role of STAT1 in CXCL10 expression (31), LPC stimulated STAT1 activating phosphorylation in PMH and induced increased CXCL10 protein levels, which were significantly reduced in PMH deficient in MLK3 (Fig. 2A). CXCL10 levels and STAT1 activated phosphorylation were also increased in PMH isolated from WT mice fed the FFC diet compared to PMH from WT mice fed the chow diet (Fig. 2A). In addition, we identified in our model that the MLK3 downstream MAPK, p38 phosphorylated activation, as well as, STAT1 phosphorylated activation and CXCL10 level were increased in Huh7 cells with LPC treatment and decreased in the presence of the MLK3 inhibitors, suggesting an MLK3/p38/STAT1 regulatory pathway in CXCL10 induction by lipotoxic stress. To further study the regulatory effect of Phospho-STAT1 on LPC induced CXCL10 upregulation, we employed a known STAT1 pharmacological inhibitor Fludarabine (flud). Fludarabine resulted in decreased LPC induced STAT1activated phosphorylation and CXCL10 protein level upregultion in Huh7 cells (Fig. 2A). Likewise, Immunogold electron microscopy for CXCL10 on EVs also displayed reduced LPC-induced CXCL10 immunogold reactivity on EVs with genetic deletion of MLK3 (Fig. 2B). We also identified an increase of CXCL10 mRNA level in Huh7 cells with LPC treatment, which was significantly reduced in the presence of the MLK3 inhibitors (Fig. 2C).

To determine the proportion of CXCL10 secreted by lipotoxic hepatocytes into EVs, the CXCL10 content in the whole conditioned media from LPC-treated Huh7 cells, the supernatant obtained after ultracentrifugation and the EVs were assessed by enzyme linked immunosorbant assay (ELISA), and demonstrated that approximately 50% of CXCL10 secreted by lipotoxic hepatocytes is in the EVs (Fig 2D). Likewise, we demonstrated that

approximately one third of CXCL10 in the serum of FFC-fed mice is associated with serum-EVs (Fig. 2E).

The increase of CXCL10 in EVs from LPC-treated hepatocytes could be due to increased cellular expression and/or trafficking into the vesicles destined for extracellular release. To differentiate between these cellular events we co-transfected Huh7 cells with GFP-tagged CXCL10 and RFP-tagged CD63, an EV marker (17). The enforced expression bypasses the need for CXCL10 induction, and permitted us to examine CXCL10 trafficking independent of its upregulation. Huh7 cells co-transfected with GFP-tagged CXCL10 and RFP-tagged CD63, displayed by both TIRF microscopy and confocal microscopy co-localization of both CXCL10 and CD63 on the cellular surface and in the extracellular vesicles, in response to LPC treatment. This co-localization was reduced in the presence of the MLK3 inhibitors (Fig. 3A). Together, these data indicate that CXCL10 enrichment in the EVs released from the lipotoxic hepatocytes is secondary to both, MLK3-induced CXCL10 upregulation and trafficking.

MLK3 is known to activate JNK, and JNK pharmacological inhibition results in a significant decrease in EVs release by lipotoxic hepatocytes (Fig. 1E). Furthermore, JNK inhibition results in retention of CXCL10 at the cellular level, and a decrease in CXCL10 trafficking into the EVs (Fig. 3B), suggesting a regulatory role of MLK3 on CXCL10 trafficking by a JNK-dependent mechanism.

Lipotoxic EVs induce macrophage chemotaxis

Because CXCL10 is a potent macrophage chemokine (32, 33), we next examined the chemotactic properties of hepatocyte-derived EVs. First, we confirmed that BMDM express CXR3, the CXCL10 cognate receptor (Fig. 4A). Next, we demonstrated that EVs isolated from LPC-treated hepatocytes increased BMDM migration in a Boyden chamber to the same extent as the recombinant mouse protein CXCL10 (rmCXCL10) at a 500 ng/ml concentration (a concentration recommended by the manufacturer to induce cell migration); this increase was attenuated by the addition of CXCL10 neutralizing antisera (Fig. 4B). The ability of an antibody to block the biological effect of CXCL10 suggests it's on the EV exterior membrane, rather than trapped in the vesicle interior. EVs derived from LPC treated *Mlk3*$^{-/-}$ hepatocytes (which are almost devoid of CXCL10) did not induce significant macrophage chemotaxis (Fig. 4C). Given that about 50% of released CXCL10 from hepatocytes is associated with EVs (Fig 2 D), we next compared the chemotactic potency of EVs to rmCXCL10 (Fig. 4D). We employed ELISA technique to measure CXCL10 contents of the EVs, and determined that EV concentration of 1×10^{11}/ml corresponds to CXCL10 concentration of 100 pg/ml). Using the same concentrations of EV-associated CXCL10 and rmCXCL10, we then showed that CXCL10 on EVs was 4 to 5 times more potent than rmCXCL10 at the same concentration in stimulating BMDM chemotaxis (Fig. 4D). Hence, EV-associated CXCL10 is more potent in stimulating chemotaxis than the free chemokine. Taken together, these data suggest that CXCL10-bearing EVs are quite potent inducers of macrophage chemotaxis.

Mlk3 genetic deficiency in a dietary NASH mouse model is associated with reduced circulating CXCL10 on Evs

To associate our *in vitro* observations with an *in vivo* correlate, we utilized our established mouse model of NASH to examine the role of EVs release in NASH pathogenesis. Mice were fed the FFC diet for 6 months. As previously reported by us, the FFC diet causes hepatocellular injury as demonstrated by elevated plasma alanine aminotransferase (ALT), levels. Also consistent with our prior observations, FFC diet-fed *Mlk3*$^{-/-}$ mice displayed reduced plasma ALT values when compared to the FFC diet-fed WT mice (Fig. 5A). Next, we examined hepatic macrophage markers in our current paradigm. We observed a significant increase in hepatic mRNA expression of macrophage surface markers in the FFC diet-fed WT mice, but not in the *Mlk3*$^{-/-}$ mice on the same diet, when normalized to chow-fed WT mice (Fig. 5B). Moreover, evidence for macrophage activation was examined by determining hepatic mRNA expression of TNF α, and IL6. Indeed, hepatic mRNA for these cytokines known to be secreted by activated macrophages were elevated in FFC diet-fed WT mice, and reduced in the *Mlk3*$^{-/-}$ mice on the same diet when normalized to chow fed WT mice (Fig. 5C). The decrease in plasma ALT values and markers of macrophage activation in *Mlk3*$^{-/-}$ mice were also associated with a decrease of plasma EV concentrations, which were significantly increased by the FFC diet in the WT mice (Fig. 5D). CXCL10 expression in the liver as assessed by mRNA, and CXCL10 levels in the total plasma and in the plasma EVs (Fig. 5E) as assessed by ELISA, demonstrated increased CXCL10 expression in liver, and CXCL10 levels in plasma and in circulating EVs of FFC-fed WT mice compared to chow-fed mice; this increase was attenuated in the FFC-fed *Mlk3*$^{-/-}$ mice. Taken together, these observations indicate that MLK3 deficiency may be salutary in steatohepatitis, in part, by reducing release of CXCL10-enriched EVs.

CXCL10 expression is increased in the liver specimen of patients with NASH

MLK3 and Phoshpo-MLK3 protein levels in liver biopsy samples from patients with normal liver histology, and patients with fatty liver were assessed by western blot. The Phospho-MLK3 antibody employed recognizes phosphorylated residues (Thr 277/Ser 281) in the activation loop of the MLK3 kinase domain. Phosphorylation of these residues is required for MLK3 kinase activity (12). We identified an increase of both total MLK3 and Phospho-MLK3 in patients with fatty liver (Supplemental figure 2A). Stimulus-mediated induction of total MLK3 protein levels has been clearly demonstrated elsewhere (12). Likewise MLK3 mRNA expression was significantly increased in patients with fatty liver compared to patients with normal liver histology (Supplemental figure 2B). In addition, CXCL10 mRNA expression was significantly increased in patient with NASH compared to normal and obese control (Supplemental figure 2C). These data suggest that patients with fatty liver have increased MLK3 protein level and likely kinase activity, with subsequent increase in CXCL10 expression.

CXL10$^{-/-}$ mice display reduced FFC-induced liver injury and inflammation

To further demonstrate the role of CXCL10 in NASH pathogenesis *in vivo* we employed *CXCL10*$^{-/-}$ mice. FFC fed *CXCL10*$^{-/-}$ mice display reduced liver injury when compared to WT mice on the same diet as demonstrated by a more favorable histology (Supplemental

figure 3A) with less steatosis and inflammatory infiltrates, and significantly lower serum ALT values (Supplemental figure 3B). These mice also have reduced hepatic macrophage infiltration as outlined by macrophage galactose-specific lectin (Mac-2) immunohistochemistry (a marker of phagocitically active macrophages) (Supplemental figure 3C). Hepatic mRNA expression of macrophage surface marker CD68 (Supplemental figure 3D) is also reduced. Taken together these data demonstrate that CXCL10 deficiency is protective against a nutrient excess diet-induced NASH in mice.

DISCUSSION

The current study provides insights regarding the mechanism by which lipotoxic hepatocyte may regulate macrophage-associated inflammatory responses during NASH. The current data indicate that: i) lipotoxic treatment of hepatocyte promotes release of CXCL10-enriched EVs via an MLK3 signaling pathway; ii) lipotoxic hepatocyte-derived EVs induce macrophage chemotaxis in a CXCL10-dependant manner; and iii) *Mlk3*$^{-/-}$ mice have decreased CXCL10-enriched circulating EVs and an associated reduction in FFC diet–induced macrophage-associated inflammation and liver injury. These findings are discussed in greater details below.

EVs are membrane-bound nanoparticles that mediate inter-cellular communication. EVs are constitutively released under physiologic conditions in different body fluids (17). Pathogenic stimuli may further increase the number of released vesicles, and may modulate their contents, as evident by increased number of circulating EVs in mouse models of ischemia reperfusion injury (34) and NASH (35). Indeed, we observed a significant increase in EVs release from hepatocytes upon treatment with toxic lipids such as palmitate and its active metabolite LPC, consistent with prior reported observations of increased release of EVs by murine hepatocytes or human hepatocyte cell line exposed to saturated free fatty acids (35). Our study extends the prior observations by elucidating, in part, the cellular mechanism driving lipotoxicity-induced EVs release. In the present study, we report that toxic lipid-mediated EVs release is MLK3-dependent. The results also suggest that MLK3 regulates the chemotactic cargo. Indeed the abundance of CXCL10 is significantly reduced in EVs derived from LPC-treated MLK3 deficient hepatocytes, or WT hepatocytes treated with LPC in the presence of the pharmacological MLK3 inhibitors. MLK3 is known to activate p38 MAPK (13, 36). STAT1 is a p38 MAPK downstream target (37). STAT1 phosphorylation, in turn, is known to increase CXCL10 expression (31, 38). Consistent with this information, we identified an increase in STAT1 phosphorylation in hepatocytes treated with LPC or isolated from FFC-fed mice, and this LPC-induced activating STAT1 and p38 phosphorylation was reduced by MLK3 pharmacologic inhibition and genetic deficiency. These observations implicate MLK3/p38/STAT1 pathway in CXCL10 induction by lipotoxic stress.

MLK3 inhibition in lipotoxic hepatocytes prevented CXCL10 localization in the vesicles, while JNK inhibition not only decreased the total number of EVs released by lipotoxic hepatocytes, but also caused retention of CXCL10 at the cellular level and reduction of CXCL10 abundance at the EV level. These opposite observations suggest that the abundance of CXCL10 in EVs released from lipotoxic hepatocytes is secondary to both, a

global induction through a STAT1-dependent mechanism, as well as to a stimulation of CXCL10 trafficking into EVs through a JNK-dependent mechanism (Fig. 6).

CXCL10 has been extensively studied in hepatitis C as a hepatocyte derived chemotactic ligand and initiator of inflammatory cascades via its cognate receptor (C-X-C motif) receptor 3 (CXCR3), which is widely expressed on Kupffer cells (the resident hepatic macrophages) and natural killer cells (39). CXCL10 is also known to attract activated monocyte-derived macrophages in different models of tissue injury (32, 33). Herein, we demonstrate that stimulation of BMDM with rmCXCL10 or CXCL10-bearing EVs induce macrophage migration in a CXCL10-dependent manner. EVs derived from WT lipotoxic hepatocyte, but not *Mlk3*$^{-/-}$ lipotoxic hepatocyte (which are almost devoid of CXCL10), induced macrophage chemotaxis, suggesting the specificity of CXCL10 in the chemotaxis process.

To extend our studies of EV release to an *in vivo* context, we utilized our nutrient excess diet-induced NASH mouse model. Interestingly MLK3 deficiency attenuated liver injury and inflammation in this model, which correlated with a decrease in CXCL10 expression in the liver, the number of circulating EVs, and their CXCL10 content. These results highlight a potential role for EVs in the pathogenesis of NASH. In addition, we demonstrated that patients with NASH have increased CXCL10 expression. Finally, because anti-CXCL10 antisera has been used in phase II clinical trial in patients with biliary cirrhosis (Study ID nct01430429; clinical trial.gov), anti-CXCL10 antisera could potentially be repurposed for the treatment of human NASH.

Although we focused on chemotaxis as opposed to macrophage activation, there are likely mediators of macrophage activation within the lipotoxic EVs. In fact, our EVs protein MS analysis demonstrated that the EVs contain numerous danger associated molecular pattern (DAMP) proteins. These DAMPs are known to elicit and activate inflammatory responses in mammalian systems (40). Thus it is likely that EVs are pro-inflammatory in addition to promoting macrophage chemotaxis into the liver. The role of DAMPs-enriched EVs as potential macrophage activators and their regulatory relationship warrants future study. The strength and hierarchal relationship between various EV cargo mediators also requires further analysis.

In summary, lipotoxicity in an MLK3-dependent manner promotes the release of CXCL10 rich lipotoxic EVs from hepatocytes, which are chemotactic for macrophages (Fig. 6). These observations provide insight into the mechanism responsible for hepatic macrophage accumulation in NASH. EVs and their cargoes, especially CXCL10, are an attractive target for developing novel therapeutic strategies for the treatment of human NASH.

Supplementary Material

Refer to Web version on PubMed Central for supplementary material.

Acknowledgments

Financial Support: This work was supported by the Center for Clinical and Translational Science (CCaTS), KL2 program KL2TR000136-09 (SHI), a Pilot and Feasibility Award (SHI), and the optical microscopy core of the Mayo Clinic Center for Cell Signaling in Gastroenterology (P30DK084567), NIH grant DK97178 (HM), NIH grant DK41876 (GJG), and the Mayo Clinic, Rochester, MN.

The authors thank Dr. B. Huang for his help in studies employing electron microscopy, Dr. A. Bamidele for his help in the study employing flow cytometry, and Eugene Krueger for his help in the study employing TIRF microcopy. We thank Dr. Cristine Charlesworth and the proteomics core at Mayo Clinic for performing the mass spectrometry analysis on the EVs. We thank B. Freeman and A. Mauer for their excellent technical assistance and C. Hoover for her excellent secretarial assistance. We thank Dr. Roger Davis, Howard Hughes Medical Institute Investigator at University of Mass Medical School for providing the *Mlk3*$^{-/-}$ mice.

List of abbreviations

MLK3	mixed lineage kinase 3
NASH	nonalcoholic steatohepatitis
EVs	extracellular vehicles
CXCL10	(C-X-C motif) ligand 10
PMH	primary mouse hepatocytes
LPC	lysophosphatidylcholine
MS	mass spectrometry
GFP	green fluorescent protein
RFP	red fluorescent protein
CD	cluster of differentiation
SFA	saturated free fatty acid
JNK	C-JUN N-terminal kinase
MAPK	mitogen-activated protein kinase
TNF	tumor necrosis factor
WT	wild type
IL	Interleukin
STAT	signal transducer and activator of transcription
PBS	phosphate buffer solution
FBS	fetal bovine serum
PA	palmitate
OA	oleate
NTA	nanoparticle tracking analysis
TIRF	total internal reflection microscopy
BMDM	bone marrow derived macrophages

DAPI	4′,6-diamidino-2-phenylindole
TSG101	tumor susceptibility gene 101
Alix	ALG-2-interacting protein
CYP2E1	cytochrome P450 2E1
flud	Fludarabine
rmCXCL10	recombinant mouse protein CXCL10
ELISA	enzyme linked immunosorbent assay
FFC	fat, fructose and cholesterol
ALT	alanine aminotransferase
CXCR3	(C-X-C motif) receptor 3
Mac-2	macrophage galactose-specific lectin
DAMP	danger associated molecular pattern
GAPDH	glyceraldehyde 3-phosphate dehydrogenase

References

1. Browning JD, Szczepaniak LS, Dobbins R, Nuremberg P, Horton JD, Cohen JC, Grundy SM, et al. Prevalence of hepatic steatosis in an urban population in the United States: impact of ethnicity. Hepatology. 2004; 40:1387–1395. [PubMed: 15565570]
2. Adams LA, Lymp JF, St Sauver J, Sanderson SO, Lindor KD, Feldstein A, Angulo P. The natural history of nonalcoholic fatty liver disease: a population-based cohort study. Gastroenterology. 2005; 129:113–121. [PubMed: 16012941]
3. Ekstedt M, Franzen LE, Mathiesen UL, Thorelius L, Holmqvist M, Bodemar G, Kechagias S. Long-term follow-up of patients with NAFLD and elevated liver enzymes. Hepatology. 2006; 44:865–873. [PubMed: 17006923]
4. Sanyal AJ. Mechanisms of Disease: pathogenesis of nonalcoholic fatty liver disease. Nature clinical practice. Gastroenterology & hepatology. 2005; 2:46–53. [PubMed: 16265100]
5. Neuschwander-Tetri BA. Hepatic lipotoxicity and the pathogenesis of nonalcoholic steatohepatitis: the central role of nontriglyceride fatty acid metabolites. Hepatology. 2010; 52:774–788. [PubMed: 20683968]
6. Feldstein AE, Canbay A, Angulo P, Taniai M, Burgart LJ, Lindor KD, Gores GJ. Hepatocyte apoptosis and fas expression are prominent features of human nonalcoholic steatohepatitis. Gastroenterology. 2003; 125:437–443. [PubMed: 12891546]
7. Han MS, Park SY, Shinzawa K, Kim S, Chung KW, Lee JH, Kwon CH, et al. Lysophosphatidylcholine as a death effector in the lipoapoptosis of hepatocytes. Journal of lipid research. 2008; 49:84–97. [PubMed: 17951222]
8. Kakisaka K, Cazanave SC, Fingas CD, Guicciardi ME, Bronk SF, Werneburg NW, Mott JL, et al. Mechanisms of lysophosphatidylcholine-induced hepatocyte lipoapoptosis. American journal of physiology Gastrointestinal and liver physiology. 2012; 302:G77–84. [PubMed: 21995961]
9. Puri P, Mirshahi F, Cheung O, Natarajan R, Maher JW, Kellum JM, Sanyal AJ. Activation and dysregulation of the unfolded protein response in nonalcoholic fatty liver disease. Gastroenterology. 2008; 134:568–576. [PubMed: 18082745]
10. Cazanave SC, Mott JL, Elmi NA, Bronk SF, Werneburg NW, Akazawa Y, Kahraman A, et al. JNK1-dependent PUMA expression contributes to hepatocyte lipoapoptosis. J Biol Chem. 2009; 284:26591–26602. [PubMed: 19638343]

11. Jaeschke A, Davis RJ. Metabolic stress signaling mediated by mixed-lineage kinases. Molecular cell. 2007; 27:498–508. [PubMed: 17679097]
12. Humphrey RK, Yu SM, Bellary A, Gonuguntla S, Yebra M, Jhala US. Lysine 63-linked ubiquitination modulates mixed lineage kinase-3 interaction with JIP1 scaffold protein in cytokine-induced pancreatic beta cell death. The Journal of biological chemistry. 2013; 288:2428–2440. [PubMed: 23172226]
13. Kim KY, Kim BC, Xu Z, Kim SJ. Mixed lineage kinase 3 (MLK3)-activated p38 MAP kinase mediates transforming growth factor-beta-induced apoptosis in hepatoma cells. J Biol Chem. 2004; 279:29478–29484. [PubMed: 15069087]
14. Amako Y, Igloi Z, Mankouri J, Kazlauskas A, Saksela K, Dallas M, Peers C, et al. Hepatitis C Virus NS5A Inhibits Mixed Lineage Kinase 3 to Block Apoptosis. J Biol Chem. 2013; 288:24753–24763. [PubMed: 23857585]
15. Ibrahim SH, Gores GJ, Hirsova P, Kirby M, Miles L, Jaeschke A, Kohli R. Mixed lineage kinase 3 deficient mice are protected against the high fat high carbohydrate diet-induced steatohepatitis. Liver Int. 2013
16. Tosello-Trampont AC, Landes SG, Nguyen V, Novobrantseva TI, Hahn YS. Kuppfer Cells Trigger Nonalcoholic Steatohepatitis Development in Diet-induced Mouse Model through Tumor Necrosis Factor-alpha Production. Journal of Biological Chemistry. 2012; 287:40161–40172. [PubMed: 23066023]
17. Raposo G, Stoorvogel W. Extracellular vesicles: exosomes, microvesicles, and friends. The Journal of cell biology. 2013; 200:373–383. [PubMed: 23420871]
18. Masyuk AI, Masyuk TV, Larusso NF. Exosomes in the pathogenesis, diagnostics and therapeutics of liver diseases. Journal of Hepatology. 2013; 59:621–625. [PubMed: 23557871]
19. Deng ZB, Liu YL, Liu CR, Xiang XY, Wang JH, Cheng ZQ, Shah SV, et al. Immature Myeloid Cells Induced by a High-Fat Diet Contribute to Liver Inflammation. Hepatology. 2009; 50:1412–1420. [PubMed: 19708080]
20. Tacke F, Zimmermann HW, Berres ML, Trautwein C, Wasmuth HE. Serum chemokine receptor CXCR3 ligands are associated with progression, organ dysfunction and complications of chronic liver diseases. Liver International. 2011; 31:842–851.
21. Zhang X, Shen JY, Man K, Chu ESH, Yau TO, Sung JCY, Go MYY, et al. CXCL10 plays a key role as an inflammatory mediator and a non-invasive biomarker of non-alcoholic steatohepatitis. Journal of Hepatology. 2014; 61:1365–1375. [PubMed: 25048951]
22. Groom JR, Luster AD. CXCR3 ligands: redundant, collaborative and antagonistic functions. Immunology and Cell Biology. 2011; 89:207–215. [PubMed: 21221121]
23. Jabeen T, Leonard P, Jamaluddin H, Acharya KR. Structure of mouse IP-10, a chemokine. Acta Crystallographica Section D-Biological Crystallography. 2008; 64:611–619.
24. Shen BY, Wu N, Yang JM, Gould SJ. Protein Targeting to Exosomes/Microvesicles by Plasma Membrane Anchors. Journal of Biological Chemistry. 2011; 286:14383–14395. [PubMed: 21300796]
25. Khalili K, Lan FP, Hanbidge AE, Muradali D, Oreopoulos DG, Wanless IR. Hepatic subcapsular steatosis in response to intraperitoneal insulin delivery: CT findings and prevalence. AJR Am J Roentgenol. 2003; 180:1601–1604. [PubMed: 12760927]
26. Webber J, Clayton A. How pure are your vesicles? Journal of extracellular vesicles. 2013:2.
27. Steyer JA, Almers W. A real-time view of life within 100 nm of the plasma membrane. Nature Reviews Molecular Cell Biology. 2001; 2:268–275. [PubMed: 11283724]
28. Nagamatsu S. TIRF microscopy analysis of the mechanism of insulin exocytosis. Endocrine Journal. 2006; 53:433–440. [PubMed: 16807501]
29. Thery, C.; Amigorena, S.; Raposo, G.; Clayton, A. Isolation and characterization of exosomes from cell culture supernatants and biological fluids. In: Bonifacino, Juan S., et al., editors. Current protocols in cell biology/editorial board. Vol. Chapter 3. 2006. p. 22
30. Uhlen M, Fagerberg L, Hallstrom BM, Lindskog C, Oksvold P, Mardinoglu A, Sivertsson A, et al. Proteomics. Tissue-based map of the human proteome. Science. 2015; 347:1260419. [PubMed: 25613900]

31. Chmielewski S, Olejnik A, Sikorski K, Pelisek J, Blaszczyk K, Aoqui C, Nowicka H, et al. STAT1-dependent signal integration between IFNgamma and TLR4 in vascular cells reflect pro-atherogenic responses in human atherosclerosis. PloS one. 2014; 9:e113318. [PubMed: 25478796]
32. Xuan WJ, Qu Q, Zheng BA, Xiong SD, Fan GH. The chemotaxis of M1 and M2 macrophages is regulated by different chemokines. Journal of Leukocyte Biology. 2015; 97:61–69. [PubMed: 25359998]
33. Petrovic-Djergovic D, Popovic M, Chittiprol S, Cortado H, Ransom RF, Partida-Sanchez S. CXCL10 Induces the Recruitment of Monocyte Derived Macrophages into Kidney, which Aggravate Puromycin Aminonucleoside Nephrosis. Clinical and experimental immunology. 2015
34. Teoh NC, Ajamieh H, Wong HJ, Croft K, Mori T, Allison AC, Farrell GC. Microparticles mediate hepatic ischemia-reperfusion injury and are the targets of Diannexin (ASP8597). PloS one. 2014; 9:e104376. [PubMed: 25222287]
35. Povero D, Eguchi A, Niesman IR, Andronikou N, du Jeu XD, Mulya A, Berk M, et al. Lipid-Induced Toxicity Stimulates Hepatocytes to Release Angiogenic Microparticles That Require Vanin-1 for Uptake by Endothelial Cells. Science Signaling. 2013:6.
36. Brancho D, Ventura JJ, Jaeschke A, Doran B, Flavell RA, Davis RJ. Role of MLK3 in the regulation of mitogen-activated protein kinase signaling cascades. Mol Cell Biol. 2005; 25:3670–3681. [PubMed: 15831472]
37. Goh KC, Haque SJ, Williams BRG. p38 MAP kinase is required for STAT1 serine phosphorylation and transcriptional activation induced by interferons. Embo Journal. 1999; 18:5601–5608. [PubMed: 10523304]
38. Sikorski K, Chmielewski S, Przybyl L, Heemann U, Wesoly J, Baumann M, Bluyssen HAR. STAT1-mediated signal integration between IFN gamma and LPS leads to increased EC and SMC activation and monocyte adhesion. American Journal of Physiology-Cell Physiology. 2011; 300:C1337–C1344. [PubMed: 21346151]
39. Brownell J, Polyak SJ. Molecular Pathways: Hepatitis C Virus, CXCL10, and the Inflammatory Road to Liver Cancer. Clinical Cancer Research. 2013; 19:1347–1352. [PubMed: 23322900]
40. Schaefer L. Complexity of danger: the diverse nature of damage-associated molecular patterns. The Journal of biological chemistry. 2014; 289:35237–35245. [PubMed: 25391648]

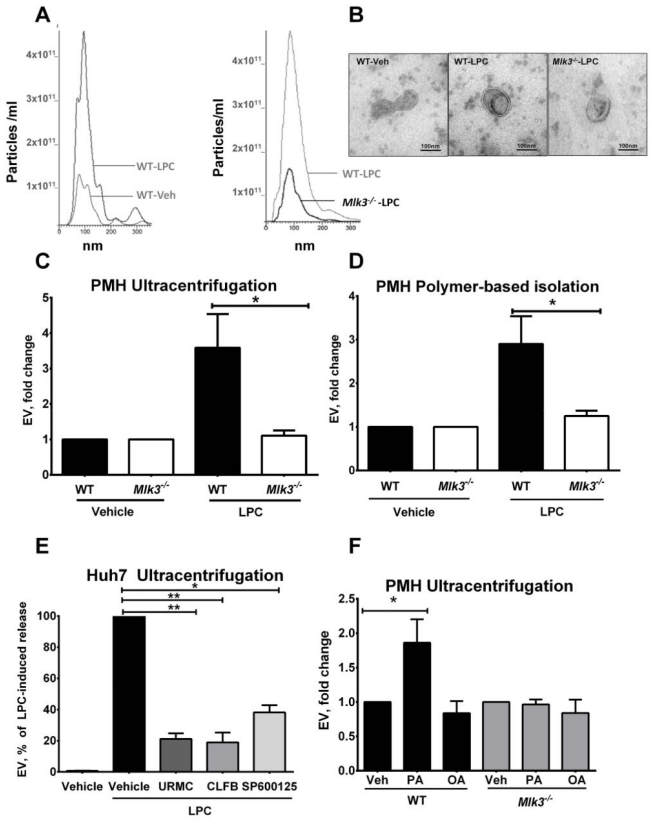

Figure 1. LPC-induced EV generation is MLK3-dependent

(A) Representative images of nanoparticle tracking analysis (NTA) profile for particle size per concentration of extracellular vesicles (EVs) released from vehicle & lysophosphatidylcholine (LPC)-treated primary mouse hepatocytes (PMH) from wild type (WT) (left panel) & mixed lineage kinase ($Mlk3)^{-/-}$ mice (right panel). (B) Representative transmission electron photomicrograph of EVs derived from vehicle and LPC-treated WT PMH and LPC-treated $Mlk3^{-/-}$ PMH, and isolated by ultracentrifugation. Fold increase above vehicle in EVs release by WT and $Mlk3^{-/-}$ PMH treated with 20 μM LPC for 4 hour, and isolated by (C) ultracentrifugation or (D) by polymer based isolation using a commercially available kit, and quantified by NTA. (E) Huh7 cells were treated with vehicle, or 20 μM LPC with or without 1 μM of one of the MLK3 inhibitors URMC099 (URMC), and CLFB1134 (CLFB), or 20 μM of C-JUN N-terminal kinase (JNK) inhibitor SP600125. EVs were isolated by ultracentrifugation, quantified using NTA, and expressed as percentage of induced LPC release. (F) PMH were treated with OA and PA (both 400 μM for 16 hours), EVs were isolated by ultracentrifugation, and quantified using NTA. Bar columns represent mean ± S.E.M. ** P < .01, * P < .05 compared to vehicle treatment

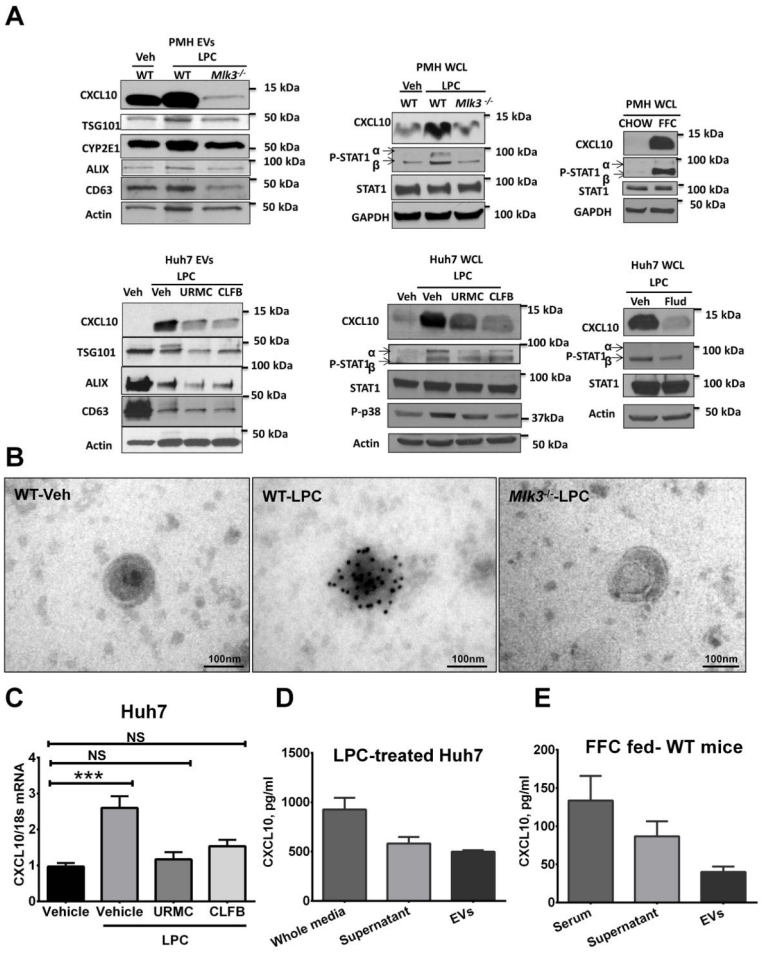

Figure 2. CXCL10 is highly expressed in lipotoxic EVs in an MLK3-dependent manner

(A) C-X-C ligand 10 (CXCL10) protein levels in extracellular vesicles (EVs) derived from wild type (WT) & mixed lineage kinase (*Mlk3*)$^{-/-}$ primary mouse hepatocytes (PMH) treated with either vehicle, or 20 μM lysophosphatidylcholine (LPC), and from Huh7 cells treated with either vehicle, or 20 μM LPC with or without 1 μM of one of the MLK3 inhibitors URMC099 (URMC) and CLFB1134 (CLFB), were assessed by western blot. Tumor susceptibility gene 101 (TSG101), cluster of differentiation (CD) 63, and ALG-2-interacting protein (Alix), were employed as EV marker and Cytochrome P450 2E1 (CYP2E1) as a marker of EVs of hepatocytes origin. CXCL10, Phospho-p38, Phospho-signal transducer and activator of transcription (PSTAT) 1 & STAT1 protein levels were also assessed by western blot on whole cell lysate from PMH and Huh7 treated with vehicle, LPC alone, or LPC in the presence of either 1 μM of one of the MLK3 inhibitors URMC, and CLFB or 100 μM of the STAT1 inhibitor Fludarabine (flud). CXCL10, P-STAT1, and STAT1 protein levels were also assessed on whole cell lysate from PMH isolated from chow, and high fat, fructose, and cholesterol diet (FFC)-fed mice, actin and glyceraldehyde 3-phosphate dehydrogenase (GAPDH) were used as loading control. (B) Immunogold reactivity for CXCL10 on EVs derived from WT & *Mlk3*$^{-/-}$ PMH was assessed by immunogold electron microscopy. (C) Total RNA was extracted from Huh7 cells treated with either vehicle, or 20 μM LPC with or without 1 μM of one of the MLK3 inhibitors

URMC099, and CLFB1134, and mRNA CXCL10 expression was evaluated by real-time qPCR. CXCL10 content was assessed (D) in the whole conditioned media of LPC-treated Huh7 cells, the supernatants obtained after ultracentrifugation and the EVs by enzyme linked immunosorbent assay (ELISA), (E) and also in the serum of FFC-fed mice, the supernatants obtained after ultracentrifugation and the EVs by ELISA. Bar columns represent mean ± S.E.M. NS (non-significant) $p > .05$, *** $P < .001$.

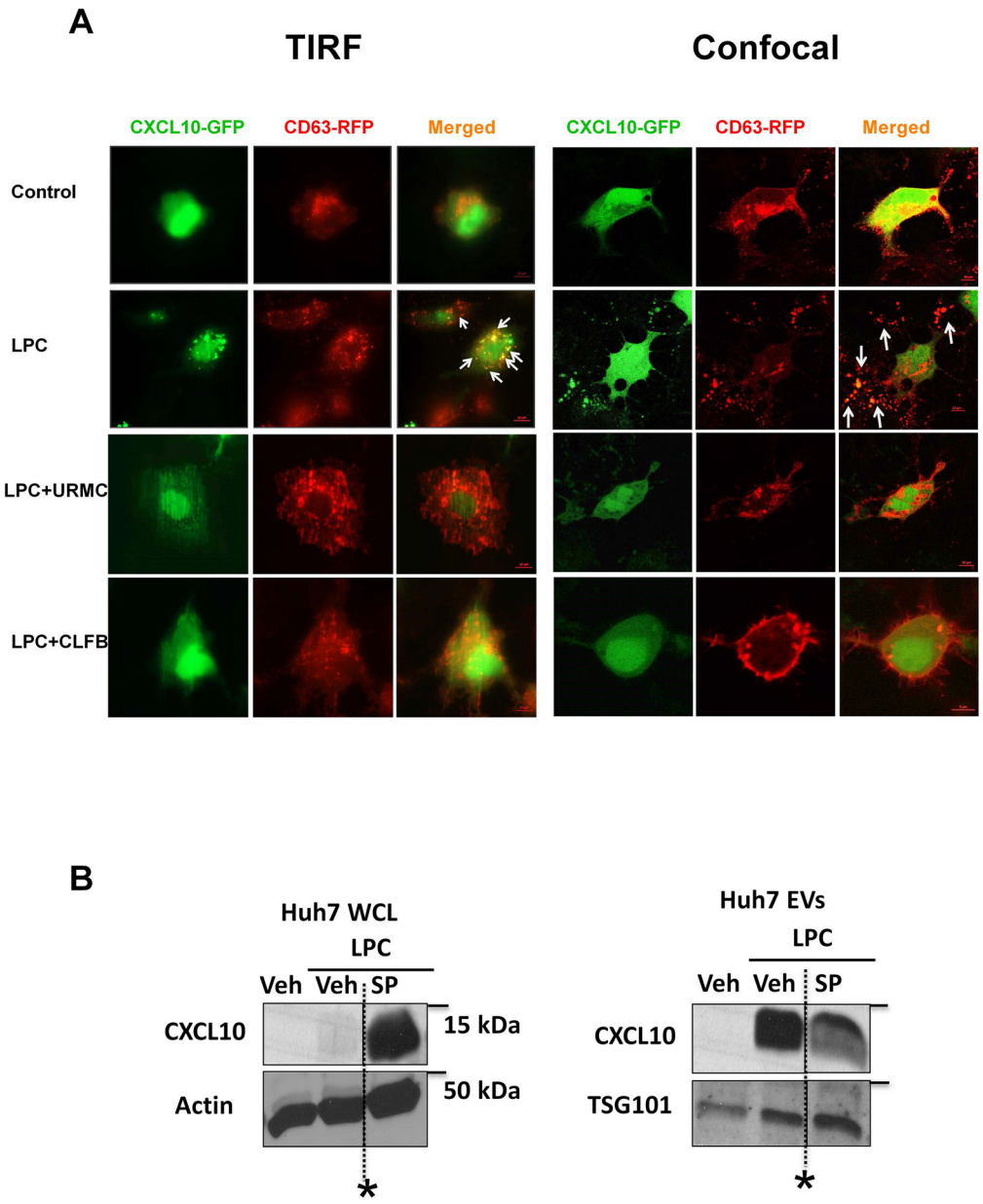

Figure 3. MLK3 mediates CXCL10 trafficking by a JNK dependent mechanism

(A) Huh7 cells were co-transfected with green fluorescent protein (GFP)-tagged C-X-C ligand chemokine 10 (CXCL10) and red fluorescent protein (RFP)-tagged cluster of differentiation (CD) 63. Co-localization of both CXCL10 and CD63 on the cell surface and in the extracellular vesicles, in response to LPC treatment with or without one of the MLK3 inhibitors URMC099, and CLFB1134, was assessed respectively by total internal reflectance microscopy (TIRF) and confocal microscopy. (B) CXCL10 protein levels in whole Huh7 cell lysate, treated with either vehicle, or 20 μM lysophosphatidylcholine (LPC) with or without 40 μM of the C-JUN N-terminal kinase (JNK), inhibitor SP600125 (SP) and in extracellular vesicles (EVs) derived from Huh 7 cells under the conditions above were

assessed by western blot. Tumor susceptibility gene 101 (TSG101) was employed as an EV marker, and actin as a loading control. (*Irrelevant bands omitted).

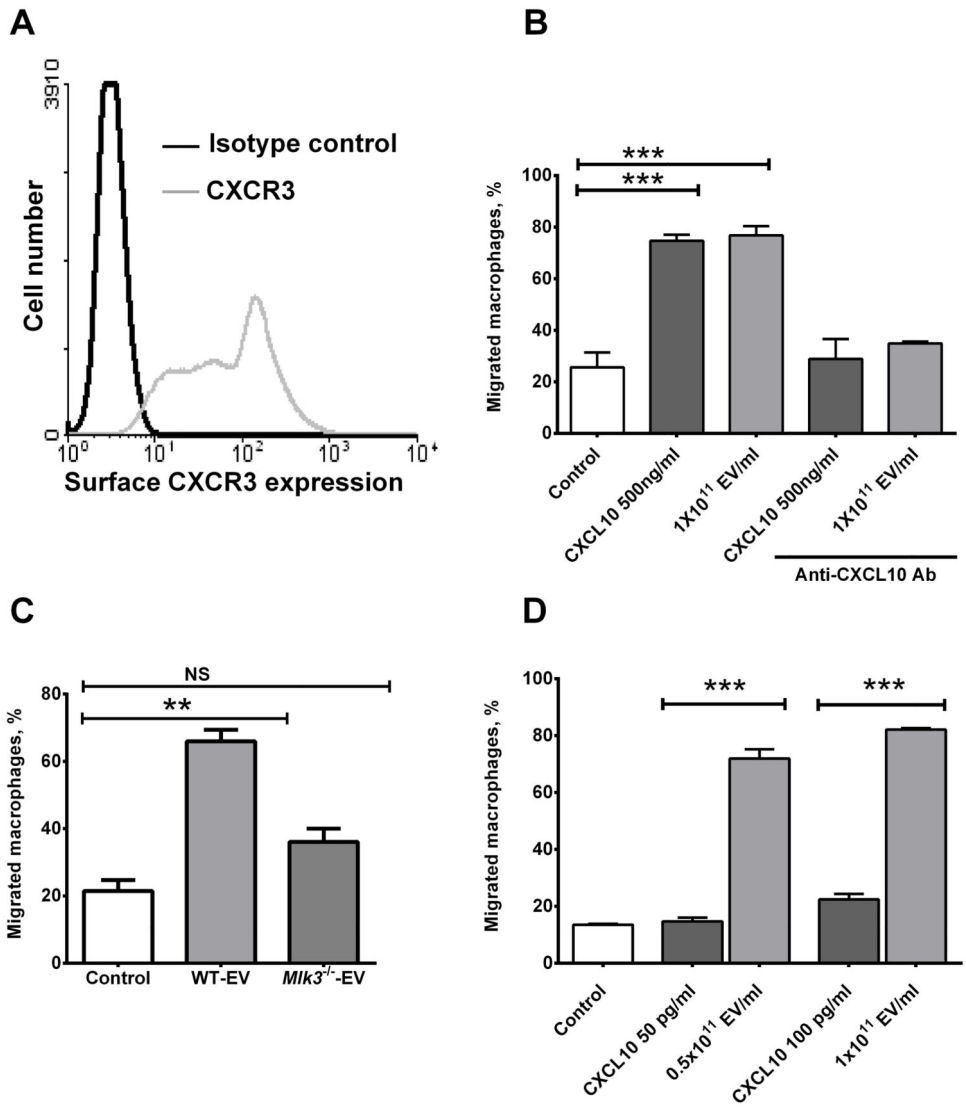

Figure 4. Lipotoxic EVs induce macrophage chemotaxis in a CXCL10-dependent manner

(A) Chemokine (C-X-C motif) receptor 3 (CXCR3) the (C-X-C motif) ligand 10 (CXCL10) cognate receptor expression was assessed on the bone marrow derived macrophages (BMDM) cell surface by flow cytometry. (B) Using a modified Boyden chamber, BMDM chemotaxis was assessed by quantification of migrating cells toward either control (media alone), extracellular vesicles (EVs) derived from lysophosphatidylcholine (LPC) treated wild type (WT) primary mouse hepatocytes (PMH) at a concentration of 10^{11} particle/ml or CXCL10 recombinant mouse protein at a concentration of 500 ng/ml with or without the CXCL10 neutralizing antibody at 25 μg/ml.(C) BMDM chemotaxis was also assessed by quantification of migrating BMDM toward either EVs derived from LPC-treated WT or *Mlk3*$^{-/-}$ PMH at a concentration of 10^{11} EV/ml. (D) 10^{11} EV/ml contain an equivalent concentration of 100 pg/ml of recombinant mouse CXCL10 (rmCXCL10) as measured by enzyme linked immunosorbent assay (ELISA). The chemotactic potency of 0.5×10^{11} EV/ml and 1×10^{11}EVs/ml were compared to an equivalent concentration of rmCXCL10 of

50 pg/ml and 100 pg/ml respectively. Bar columns represent mean ± S.E.M. *** P < .001, ** P < .01 compared to vehicle treatment.

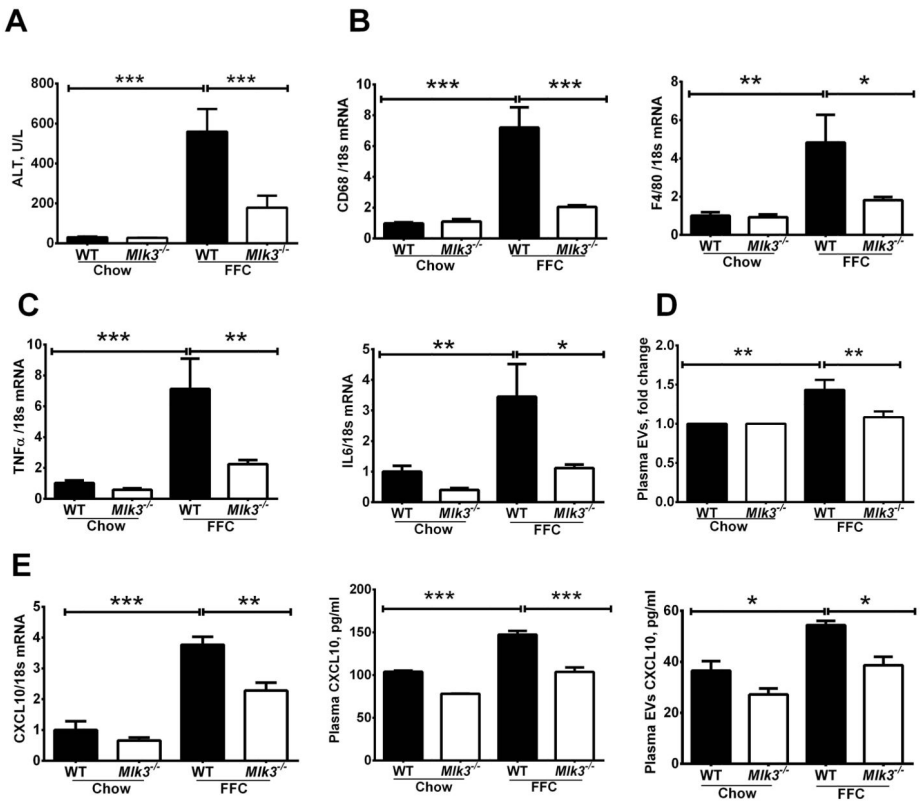

Figure 5. *Mlk3*$^{-/-}$ mice are protected against high fat, fructose and cholesterol (FFC) diet-induced liver injury and inflammation and have reduced plasma level of CXCL10 enriched extracellular vesicles (EVs)

Wild type (WT) & mixed lineage kinase *(Mlk3)*$^{-/-}$ mice were fed either chow or FFC diet. (A) Plasma alanine aminotransferase (ALT) levels were measured. Total RNA was extracted from liver tissue and mRNA expression of (B) surface macrophage markers cluster of differentiation (CD) 68 and F4/80, (C) macrophage cytokines tumor necrosis factor (TNF) α, and interleukin (IL) 6, and (E) CXCL10 expression were evaluated by real-time qPCR. (D) Enzyme linked immunosorbant assay (ELISA) for (C-X-C motif) ligand 10 (CXCL10) was performed on (E) the whole plasma and EVs isolated from the plasma of FFC and chow fed WT and *Mlk3*$^{-/-}$ mice. Bar columns represent mean ± S.E.M. *** P < .001, ** P < .01, * P < .05 compared to WT chow-fed mice

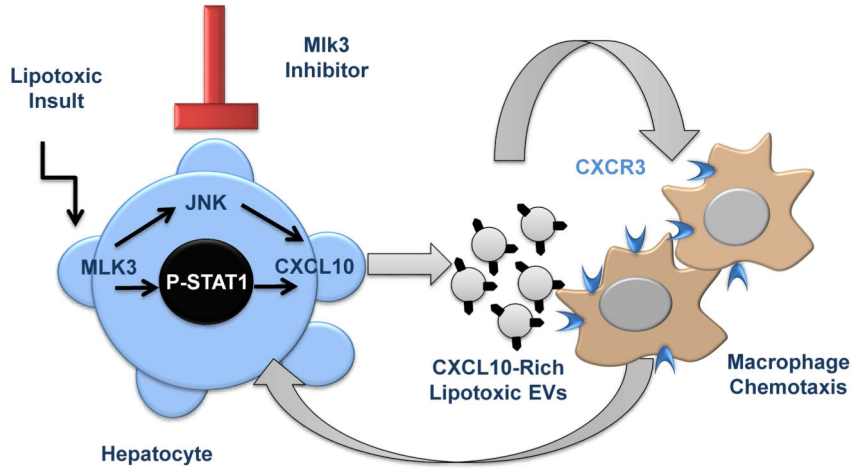

Figure 6. Schematic diagram illustrating the link between lipotoxic hepatocytes and macrophages trafficking to the liver in NASH

Lipotoxicity during NASH promotes the release of (C-X-C motif) ligand 10 (CXCL10)-bearing extracellular vesicles (EVs) from hepatocytes by a mixed lineage kinase (MLK)3-dependant mechanism that involves CXCL10 induction through a STAT1-dependent mechanism, and CXCL10 trafficking into EVs through a C-JUN N-terminal kinase (JNK)-dependent mechanism. CXCL10-enriched EVs mediate macrophage chemotaxis to the liver. MLK3 inhibition prevents CXCL10-enriched EVs release from hepatocytes and thus attenuates macrophage chemotaxis.

Table 1

Primer sequences for quantitative real-time PCR

Gene	Forward primer sequence (5′–3′)	Reverse primer sequence (5′–3′)
18S	CGC TTC CTT ACC TGG TTG AT	GAG CGA CCA AAG GAA CCA TA
mouse		
CXCL10	CCA AGT GCT GCC GTC ATT TTC	GGC TCG CAG GGA TGA TTT CAA
TNFα	CCC TCA CAC TCA GAT CAT CTT CT	GCT ACG ACG TGG GCT ACA G
IL-1β	GCA ACT GTT CCT GAA CTC AAC T	ATC TTT TGG GGT CCG TCA ACT
IL-6	TAG TCC TTC CTA CCC CAA TTT CC	TTG GTC CTT AGC CAC TCC TTC
F4/80	ATG GAC AAA CCA ACT TTC AAG GC	GCA GAC TGA GTT AGG ACC ACA A
CD68	TGT CTG ATC TTG CTA GGA CCG	GAG AGT AAC GGC CTT TTT GTG A
human		
MLK3	GCAGCCCATTGAGAGTGAC	CACTGCCCTTAGAGAAGGTGG
CXCL10	GTC GCA TTC AAG GAG TAC CTC	TGA TGG CCT TCG ATT CTG GAT T